J Therm Anal Calorim (2012) 107:1251–1257
DOI 10.1007/s10973-011-1778-0

Thermal degradation kinetics of semi-aromatic polyamide containing benzoxazole unit

Hongbo Gu · Jin Mei He · Jun Hu · Yu Dong Huang

Received: 15 March 2011 / Accepted: 28 June 2011 / Published online: 30 July 2011

Abstract The kinetics of the thermal degradation of a new semi-aromatic polyamide containing benzoxazole unit (BO6) have been investigated by thermogravimetric analysis (TG). Thermal degradation of BO6 could be accomplished by one step. The corresponding kinetic parameters of the degradation process are determined by using Kissinger and Flynn–Wall–Ozawa methods, respectively. Coats–Redfern method is also used to discuss the probable degradation mechanism of the BO6. The results show that the activation energy obtained from Kissinger method is in good agreement with the value obtained by using Flynn–Wall–Ozawa method. The solid-state degradation mechanism of the BO6 is a decelerated R_1 type (phase boundary controlled reaction one-dimensional movement).

Keywords Semi-aromatic polyamide · Benzoxazole · Thermal degradation · Kinetic analysis · Thermogravimetric analysis

Introduction

Aliphatic polyamides such as PA6, PA66, and PA1010 possess a favorable balance of physical and chemical properties, which has been widely used as engineering materials [1–3]. However, their thermal stability is very poor due to the low melting point and/or glass transition temperature, which limit their application at high temperature. In our study, a new semi-aromatic polyamide (BO6) containing benzoxazole unit based on 5-amino-2-(*p*-aminophenyl) benzoxazole (ABO) and adipic acid has been successfully synthesized to improve the thermal property. The results have shown that the chemical nature of the benzoxazole group has effects on the degradation of polyamide [4]. The investigation on the thermal degradation kinetics and mechanism of BO6 must be fully understood for successful use in manufacture and elevated temperature applications.

Thermogravimetric analysis (TG) has been widely used to determine the kinetic parameters of the degradation process, such as activation energies (E) and reaction orders (n), etc. [5–10]. Kinetic data could help us to understand the thermal degradation mechanism [11].

In this article, the thermal degradation of BO6 has been investigated with TG analysis. One objective is to study the activation energy (E), reaction order (n), and frequency factor (A) of BO6 by using different heating rates under nitrogen conditions. The other is to study the thermal degradation mechanism as a solid-state process.

Theoretical background

In general, the thermal degradation reaction of a solid polymer could be described as:

$$A_{\text{solid}} = B_{\text{solid}} + C_{\text{gas}} \tag{1}$$

It means that a solid polymer A (solid) is decomposed into residue B (solid) and volatile substances C (gas). In TG measurements, the degree of decomposition could be calculated as follows [12]:

$$X = \frac{W_0 - W_t}{W_0 - W_\infty} \tag{2}$$

where X is the degree of decomposition; W_0, W_t, W_∞ represent the initial, actual, and final mass of the material,

H. Gu · J. M. He · J. Hu · Y. D. Huang (✉)
School of Chemical Engineering and Technology, Harbin Institute of Technology, PO Box 410, Harbin 150001, China
e-mail: ydhuang.hit1@yahoo.com.cn

respectively. A typical model for the decomposition degree of the polymer A could be shown as:

$$\frac{dX}{dt} = k \cdot f(X) \tag{3}$$

where dX/dt represents the decomposition rate; $f(X)$ stands for the function of X. And k is the Arrhenius rate constant:

$$k = A \cdot \exp(-E/RT) \tag{4}$$

where E is the activation energy (J mol^{-1}), R is the gas constant (8.314 J mol^{-1} K^{-1}), A is the frequency factor (M^{1-n} s^{-1}), and T is Kelvin temperature (K). Substituting the Eq. 4 into Eq. 3, we could obtain

$$\frac{dX}{dt} = A \cdot \exp(-E/RT) \cdot f(X) \tag{5}$$

under the constant heating rate β ($\beta = dT/dt$, °C min^{-1}), the degree of decomposition could be analyzed as follows:

$$\frac{dX}{dT} = \frac{A}{\beta} \cdot \exp(-ET/RT) \cdot f(X) \tag{6}$$

The Eq. 5 and Eq. 6 are the basic equations for the kinetic calculation.

Kissinger method [13]

The Kissinger equation is:

$$\ln\left(\frac{\beta}{T_p^2}\right) = \ln\frac{AR}{E} + \ln\left[n(1-X_p)^{n-1}\right] - \frac{E}{RT_p} \tag{7}$$

where β is the heating rate, T_p is the maximum temperature of loss rate on the TG curves, A is the frequency factor, X_p is the conversion rate of the maximum mass loss rate, and n is the reaction order. The activation energy (E) could be calculated from the slope coefficient of the straight line by plotting $\ln(\beta/T_p^2)$ against $1{,}000/T_P$.

Flynn–Wall–Ozawa method [14, 15]

Separating the variable Eq. 6, it could be obtained:

$$g(X) = \int_{X_0}^{X_p} \frac{dX}{f(X)} = \frac{A}{\beta}\int_{T_0}^{T_p} \exp(-E/RT)dT \tag{8}$$

Defining $x = E/RT$ and integrating the right-hand side of Eq. 8, it could be obtained:

$$\frac{A}{\beta}\int_{T_0}^{T_p} \exp(-E/RT)dT = \frac{AE}{\beta T}p(x) \tag{9}$$

Substituting the Eq. 9 into the Eq. 8, and then calculating the logarithms, the result could be expressed as:

$$\log\beta = \log\frac{AE}{g(X)R} + \log p(x) \tag{10}$$

where

$$p(x) = \left(e^{-x}/x^2\right)\sum_{n=1}(-1)^{n-1}\left(n!/x^{n-1}\right)$$

and $g(x)$ is the function of the decomposition degree. When $20 \le x \le 60$ is true, using the Doyle approximation, $p(x)$ could be expressed approximately:

$$\log p(x) \approx -2.315 - 0.4567x \tag{11}$$

Substituting the Eq. 11 into the Eq. 10 and rearranging, we could obtain:

$$\log\beta = \log\frac{AE}{g(X)R} - 2.315 - \frac{0.4567E}{RT} \tag{12}$$

From this equation, $\log\beta \sim 1{,}000/T$ is a straight line, the activation energy (E) could be obtained from the slope coefficient ($-0.4567E/R$).

Coats—Redfern method [16, 17]

Coats—Redfern method solves the Eq. 8 by using an asymptotic approximation at the different conversion rates. If $(2RT)/E \to 0$ is true for the Doyle approximation, we could obtain a natural logarithmic formula:

$$\ln\frac{g(X)}{T^2} = \ln\frac{AR}{\beta E} - \frac{E}{RT} \tag{13}$$

According to the different degradation processes, the corresponding theoretical function $g(X)$ is listed in Table 1 [18]. Activation energy (E) could be calculated by the plot of $\ln[g(X)/T^2] \sim 1/T$, by comparing, with which the activation energies from Kissinger method and Flynn–Wall–Ozawa method, and the reaction mechanism could be determined.

Experimental

Materials

ABO (from Standard Chemicals, Tianjing, China), as aromatic diamine, was used as-received without any further treatment. Adipic acid (from Guangfu Fine Chemicals, Tianjing, China), as aliphatic diacids, were used after recrystallization. *N*-methyl-2-pyrrolidone (NMP) (from Standard Chemicals, Tianjing, China) was purified by vacuum distillation and stored in the presence of molecular sieves. Pyridine (Py) (from Xinxi Reagents, Tianjing, China) was distilled and stored over KOH pellets before using. Triphenyl phosphite (TPP) (from Guangfu Fine

Table 1 Algebraic expressions for $g(X)$ for the mechanisms of solid-state processes [18]

Symbol	$g(X)$	Solid-state processes
Sigmoidal curves		
A_2	$[-\ln(1-X)]^2$	Nucleation and growth (Avrami equation 1)
A_3	$[-\ln(1-X)]^3$	Nucleation and growth (Avrami equation 2)
A_4	$[-\ln(1-X)]^4$	Nucleation and growth (Avrami equation 3)
Deceleration curves		
R_1	X	Phase boundary controlled reaction (one-dimensional movement)
R_2	$2[1-\ln(1-X)^{1/2}]$	Phase boundary controlled reaction (contracting area)
R_3	$3[1-\ln(1-X)^{1/3}]$	Phase boundary controlled reaction (contracting volume)
D_1	X^2	One-dimensional diffusion
D_2	$(1-X)\ln(1-X)+X$	Two-dimensional diffusion (Valensi equation)
D_3	$[1-(1-X)^{1/3}]^2$	Three-dimensional diffusion (Jander equation)
D_4	$[1-(2/3)X]-(1-X)^{2/3}$	Three-dimensional diffusion (Ginstling–Brounshtein equation)
F_1	$-\ln(1-X)$	Random nucleation with one nucleus on the individual particle
F_2	$1/(1-X)$	Random nucleation with two nuclei on the individual particle
F_3	$1/(1-X)^2$	Random nucleation with three nuclei on the individual particle

Chemicals, Tianjing, China) as the catalyzer, was purified by washing successively with 5 wt% aqueous NaOH, then distilled water, and finally with saturated NaOH solution, followed by drying over anhydrous $MgSO_4$. Lithium chloride (LiCl) (Standard Chemicals, Tianjing, China) was dried under vacuum at 160 °C for 5 h.

Preparation of BO6

A typical procedure for the preparation of BO6 was taken as follows: a 100 mL four-necked flask, equipped with polytetrafluoroethylene stirrer, nitrogen inlet, thermometer, and reflux condenser, respectively, was charged with 5 mmol (0.730 g) adipic acid, 5 mmol (1.125 g) aromatic diamine, 13 mmol (3.3 mL, 3.880 g) triphenyl phosphate, 6.3 mmol (0.267 g) lithium chloride, 37.2 mmol (3 mL, 2.948 g) Py, and 123.7 mmol (12 mL, 12.336 g) NMP. The mixture was heated for 5 h in a thermostatically controlled heater at 90 °C under stirring and mild nitrogen purging. When the polymerization was finished, the reaction mixture was poured into 100 mL methanol to precipitate the polymer, which was collected by filtration. The polymer was agitated in 25 mL hot ethanol for 10 min, and filtered again. The washing treatment was repeated three times, and the product was finally dried under vacuum (−0.09 MPa, 100 °C, 10 h). The polymerization process is shown in Scheme 1.

TG analysis

TG analysis was obtained on a Pyris PE system at various heating rate of β (10, 15, 20, 25, 30 °C min^{-1}) under nitrogen atmosphere from 20 to 600 °C.

Results and discussion

Thermal degradation kinetics of BO6

The TG curves and differential TG (DTG) curves of BO6 at different heating rates in nitrogen are shown in Figs. 1 and 2.

The calculation of activation energy (E)

According to the Kissinger equation, the fitting correlation coefficient R is 0.98658 by the plot of $\ln(\beta/T_p^2)$ against $1{,}000/T_p$, as shown in Fig. 3. The activation energy (E) is 210.69 kJ mol^{-1} is calculated by the slope coefficient of the straight line.

Scheme 1 Process of the polymerization

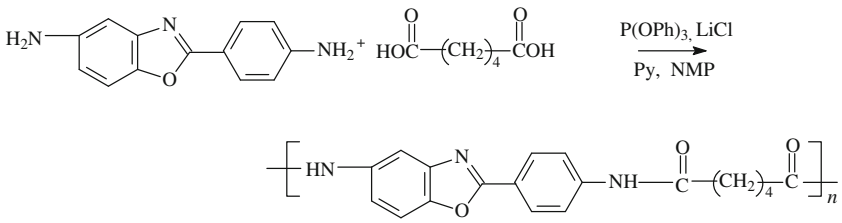

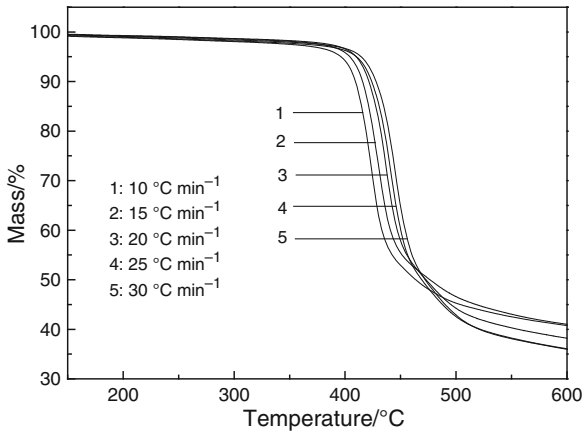

Fig. 1 TG curves of BO6 at different heating rates in N_2

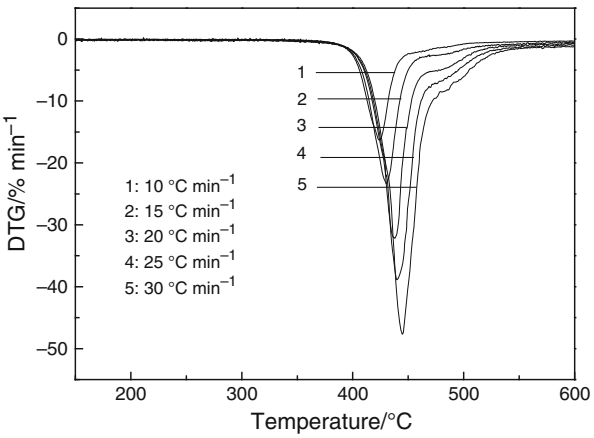

Fig. 2 DTG curves of BO6 at different heating rates in N_2

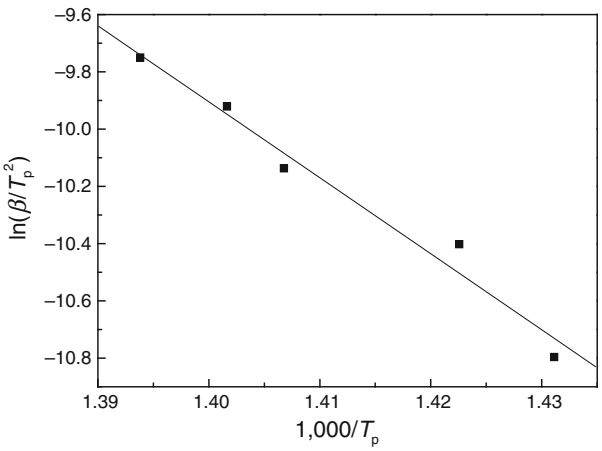

Fig. 3 Plot of $\ln(\beta/T_p^2)$ against $1{,}000/T_p$ according to Kissinger's equation

Flynn–Wall–Ozawa method is an integral method. The curves of conversion (X) versus temperature at different heating rates are shown in Fig. 4. $X = 0.2$, 0.25, 0.30, 0.35, 0.40, 0.45, 0.50, 0.55, 0.60, and 0.65 are taken to evaluate activation energy, respectively. According to the Eq. 12, the activation energy (E) could be obtained from the slope coefficient ($-0.4567E/R$) by the plot of $\log\beta$ versus $1{,}000/T$, as shown in Fig. 5. The slope coefficient and correlation coefficient at different conversion (X) are listed in Table 2. Finally, the average activation energy of BO6 is 200.53 kJ mol^{-1}.

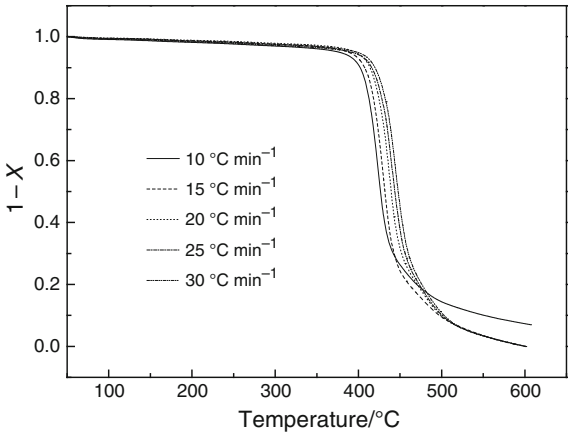

Fig. 4 Curves of conversion degree versus temperature at different heating rates

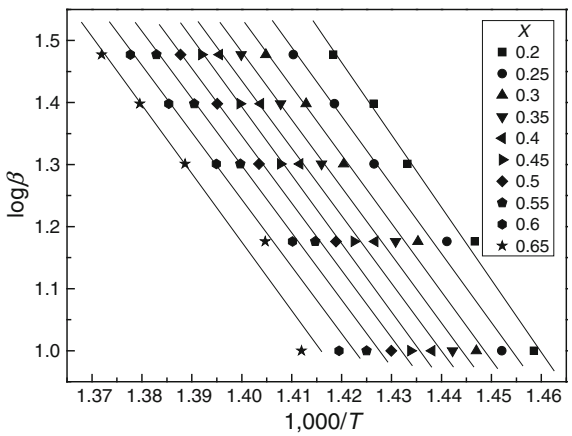

Fig. 5 Fitted curves at different conversions

It could be concluded from the activation energy (E) obtained by the two methods that the results are close to each other. Therefore, it means that the determination of activation energy (E) from Kissinger equation and Flynn–Wall–Ozawa method is reliable.

The determination of reaction order (n) and frequency factor (A)

For the simple reaction, the simplest and most commonly used model of $f(X)$ is as follows [19]:

Table 2 Slope coefficient and correlation coefficient at different conversions

X	Slope coefficient	E/kJ mol^{-1}	Correlation coefficient/R
0.20	−11.68919	212.79	0.99653
0.25	−11.09544	201.98	0.99430
0.30	−11.01261	200.47	0.99536
0.35	−10.92453	198.87	0.99492
0.40	−10.88596	198.16	0.99463
0.45	−11.02609	200.71	0.99495
0.50	−10.84727	197.46	0.99390
0.55	−10.82714	197.09	0.99224
0.60	−10.81172	196.81	0.98949
0.65	−11.03767	200.93	0.98323

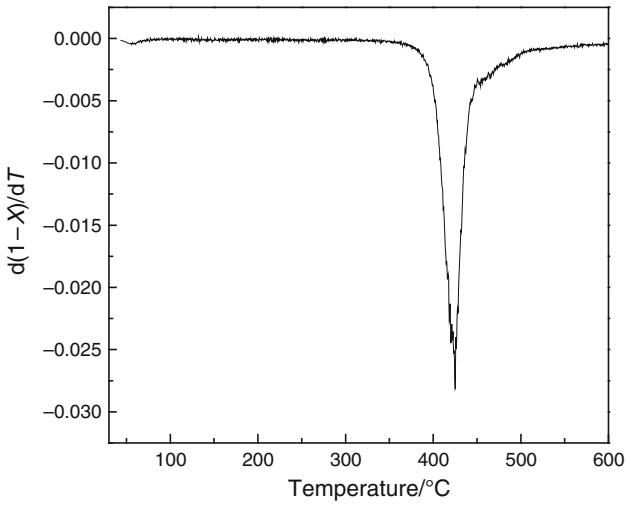

Fig. 6 Differential curve of TG at 10 °C min^{-1}

$$f(X) = (1 - X)^n \tag{14}$$

Substituting the Eq. 13 into the Eq. 6, rearranging and calculating the natural logarithm, we could obtain:

$$\ln[(\beta \mathrm{d}X/\mathrm{d}T)/\exp(-E/RT)] = \ln A + n\ln(1 - X) \tag{14}$$

The reaction order (n) and frequency factor (A) could be obtained from the slope coefficient and intercept by the plot of $\ln[(\beta \mathrm{d}X/\mathrm{d}T)/\exp(-E/RT)]$ versus $\ln(1 - X)$.

The differential curve of TG at 10 °C min^{-1} is shown in Fig. 6. $X = 0.50$, 0.55, 0.60, 0.65, 0.70, and 0.75 are chosen to calculate the $\ln[(\beta \mathrm{d}X/\mathrm{d}T)/\exp(-E/RT)]$. The results are listed in Table 3.

The fitting line of $\ln[(\beta \mathrm{d}X/\mathrm{d}T)/\exp(-E/RT)]$ against $\ln(1 - X)$ is shown in Fig. 7. It is found that the reaction order (n) is 2.98126. The frequency factor (A) is 2.29405 M$^{-1.98126}$ s^{-1}.

Table 3 Values at different conversions

X	T/K	$\ln(1 - X)$	$\ln[(\beta \mathrm{d}X/\mathrm{d}T)/\exp(-E/RT)]$
0.50	699.34	−0.69310	−1.35943
0.55	701.71	−0.79850	−1.48157
0.60	704.48	−0.91630	−1.79897
0.65	708.23	−1.04982	−2.24189
0.70	714.59	−1.20397	−2.88132
0.75	726.85	−1.38629	−3.28551

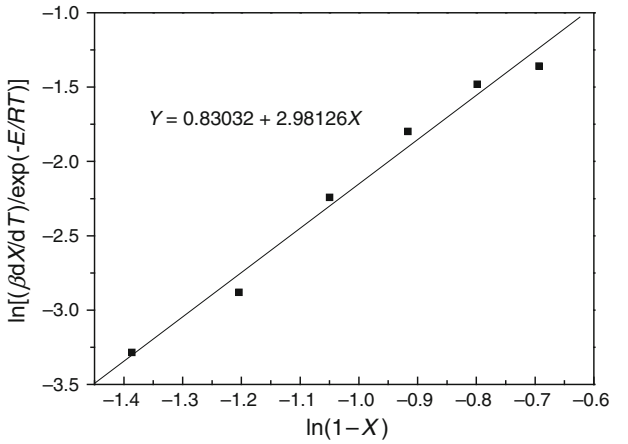

Fig. 7 Reaction order (n) and the frequency factor (A) from experimental data

Kinetic mechanism of BO6

To investigate the solid-state process for the thermal degradation of BO6, Coats—Redfern method is chosen as it involved the mechanism of solid-state process.

According to the Eq. 13, the activation energy (E) for every $g(X)$ function listed in Table 1 could be obtained from the slope coefficient by the plot of $\ln[g(X)/T^2]$ versus $1/T$. $X = 0.20$, 0.25, 0.30, 0.35, 0.40, 0.45, 0.50, 0.55, 0.60, 0.65, 0.70, 0.75, and 0.80 are taken to calculate the activation energy (E), and correction coefficient of every $g(X)$ function at a heating rate ($\beta = 10$ °C min^{-1}). The fitted curves at different conversion of Coats–Redfern method are shown in Fig. 8. And the calculated results are listed in Table 4.

Compared with the activation energy (E) obtained from Kissinger equation and Flynn–Wall–Ozawa method, the same result is obtained in Coats—Redfern method. When the thermal degradation mechanism for BO6 is a R_1 type, the activation energy (E) corresponds to the other two methods. Therefore, the R_1 type is probably the thermal degradation kinetic mechanism, and the rate-controlling process of thermal degradation of BO6 followed the phase boundary controlled reaction one-dimensional movement (R_1) with the integral form $g(X) = X$. In phase boundary-controlled

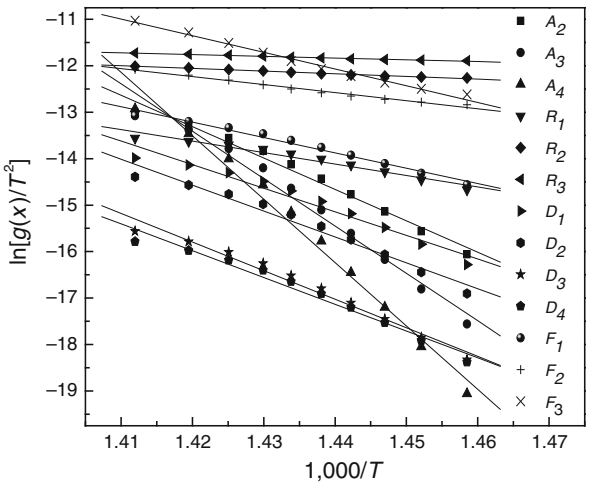

Fig. 8 Fitted curves at different conversion of Coats–Redfern method

Table 4 Activation energies for different mechanisms

Mechanism	Slope coefficient	E/kJ mol^{-1}	Correlation coefficient/R
A_2	−67.53898	561.49	0.99138
A_3	−102.00520	848.03	0.99150
A_4	−136.47142	1134.57	0.99155
R_1	−24.69409	205.30	0.99384
R_2	−5.78093	48.06	0.99494
R_3	−3.78221	31.44	0.99281
D_1	−50.78164	422.47	0.98187
D_2	−55.76520	463.61	0.98537
D_3	−61.53163	511.55	0.98875
D_4	−57.67897	479.52	0.98662
F_1	−33.07277	274.95	0.99100
F_2	−17.26811	143.56	0.99295
F_3	−35.92967	298.70	0.99347

reactions, the reaction is controlled by movement of an interface at constant velocity and then equation relating X is the R_1 function for a movement along a straight line [20].

Conclusions

The kinetic parameters of the thermal degradation of BO6 are investigated by using different methods. The results show that the activation energy (E) obtained from Kissinger and Flynn–Wall–Ozawa methods are 210.69 and 200.53 kJ mol^{-1}, respectively. The reaction order (n) and frequency factor (A) calculated by the differential are 2.98126 and 2.29405 $M^{-1.98126}$ s^{-1}, respectively. The result from Coats–Redfern method illustrates that the solid-state process for the thermal degradation of BO6 obeys the phase boundary controlled reaction one-dimensional movement (R_1) with the integral form $g(X) = X$.

Acknowledgements The authors would like to thank the Changjiang Scholars Program. The authors also thank Prof. Zhang for the availability of the TG facility at the Center of the Chemical Laboratory in Northeast Forestry University.

References

1. Huang CC, Chang FC. Reactive compatibilization of polymer blends of poly(butylene terephthalate) and polyamide 6,6: 2 morphological and mechanical properties. Polymer. 1997;38(17):4287–93.
2. Colin AF, Leslie HR, Nick EB. Water penetration in nylon 6,6: absorption desorption, and exchange studied by NMR microscopy. J Polym Sci A Polym Chem. 1993;31(1):159–68.
3. Yeong CY, Won HJ. Segmented block copolyetheramides based on nylon 6 and polyoxypropylene. I. Synthesis and characterization. J Appl Polym Sci. 1994;54(5):585–91.
4. Hu J, He JM, Gu HB, Oiu JH, Huang YD, Sun DZ. Synthesis and characterization on semi-aromatic polyamide containing benzoxazole unit. J Harbin Inst Technol. 2011;18(3):95–100.
5. Jin WP, Sea CO, Hac PL, Hee TK, Kyong OY. A kinetic analysis of thermal degradation of polymers using a dynamic method. Polym Degrad Stab. 2000;67:535–40.
6. Yang KK, Wang XL, Wang YZ, Wu B, Yin YD, Yang B. Kinetics of thermal degradation and thermal oxidative degradation of poly(*p*-dioxanone). Eur Polym J. 2003;39:1567–74.
7. Korkut A. Thermogravimetric analysis of walnut shell as pyrolysis feedstock. J Therm Anal Calorim. 2010;105(1):145-50.
8. Mostashari SM, Baie S. TG studies of synergism between red phosphorus (RP)—calcium chloride used in flame-retardancy for a cotton fabric favorable to green chemistry. J Therm Anal Calorim. 2010;99:431–6.
9. Sovizi MR, Anbaz K. Kinetic investigation on thermal decomposition of organophosphorous compounds. *N*,*N*-dimethyl-*N*′,*N*′-diphenylphosphorodihydrazidic and diphenyl amidophosphate. J Therm Anal Calorim. 2010;99:593–8.
10. Anca MM, Lucia O, Apostolescu N, Moldoveanu C. TG-FTIR study on thermal degradation in air of some new diazoamino derivatives. J Therm Anal Calorim. 2010;100:615–22.
11. Sun JT, Huang YD, Gong GF, Cao HL. Thermal degradation kinetics of poly(methylphenylsiloxane) containing methacryloyl groups. Polym Degrad Stab. 2006;91:339–46.
12. Nam JD, Seferis JC. Generalized composite degradation kinetics for polymeric systems under isothermal and nonisothermal condition. J Polym Sci B Polym Phys. 1992;30:455–63.
13. Kim SW, Chao YS, Shim MJ. Thermal degradation kinetics of PE by the Kissinger equation. Mater Chem Phys. 1998;52(1):94–7.
14. Popescu C. Integral method to analyze the kinetics of heterogeneous reactions under non-isothermal conditions a variant on the Ozawa–Flynn–Wall method. Thermochim Acta. 1996;285:309–23.
15. Bonnet E, White RL. Species-specific isoconversion effective activation energies derived by thermogravimetry—mass spectrometry. Thermochim Acta. 1998;311(1):81–6.
16. Mu P, Wang RF, Zhao L. Studies on the non-isothermal kinetics of thermal decomposition process of the complex of europium *p*-methylbenzoate with 2,2′-dipyridine. Thermochim Acta. 1997;296(1):129–34.
17. Tomaszewicz E, Kotfica M. Mechanism and kinetics of thermal decomposition of nickel(II) sulfate(VI) hexahydrate. J Therm Anal Calorim. 2004;77(1):25–31.

18. Urbanovici E, Popescu C. Improved iterative version of the Coats–Redfern method to evaluate non-isothermal kinetic parameters. J Therm Anal Calorim. 1999;58:683–700.
19. Li LQ, Guan CX, Zhang AQ, Chen DH, Qing ZB. Thermal stabilities and thermal degradation kinetics of polyimides. Polym Degrad Stab. 2004;84(3):369–73.
20. Mahfouz RM, Al-Shehri SM, Monshi MAS, Alhaizan AI, El-Salam NM. Isothermal decomposition of γ-irradiated erbium acetate. Defects Solids. 2007;162(2):95–100.